Eur. Phys. J. B **27**, 527–540 (2002)
DOI: 10.1140/epjb/e2002-00186-9

THE EUROPEAN PHYSICAL JOURNAL B

Mixed valence on a pyrochlore lattice – LiV_2O_4 as a geometrically frustrated magnet

N. Shannon[a]

Max–Planck–Institut für Physik komplexer Systeme, Nöthnitzer Str. 38, 01187 Dresden, Germany

Received 12 March 2002 and Received in final form 3 May 2002
Published online 25 June 2002 –

Abstract. Above 40 K, the magnetic susceptibility of the heavy Fermion spinel LiV_2O_4 has many features in common with those of geometrically frustrated magnetic insulators, while its room temperature resistivity comfortably exceeds the Mott-Regel limit. This suggests that local magnetic moments, and the underlying geometry of the pyrochlore lattice, play an important role in determining its magnetic properties. We extend a recently introduced tetragonal mean field theory for insulating pyrochlore antiferromagnets to the case where individual tetrahedra contain spins of different lengths, and use this as a starting point to discuss three different scenarios for magnetic and electronic transitions in LiV_2O_4.

PACS. 71.27.+a Strongly correlated electron systems; heavy fermions – 71.10.-w Theories and models of many-electron systems – 75.40.Cx Static properties (order parameter, static susceptibility, heat capacities, critical exponents, etc.)

1 Introduction

Geometrically frustrated magnetic insulators continue to fascinate experimental and theoretical physicist alike. These systems are intriguing because the physics of a wide range of materials, with an equally wide range of physical properties, is underpinned by alluringly simple considerations of symmetry and entropy. Perversely, the properties of frustrated systems which are structurally far more complicated than "textbook" magnetic insulators can therefore sometimes be understood on the basis of very simple arguments [1].

Recently, the geometrically frustrated "metal" LiV_2O_4 has also attracted a great deal of attention as the first example of d-electron heavy Fermion system. In this article we apply simple arguments borrowed from the study of frustrated magnetic insulators to the magnetic susceptibility of LiV_2O_4 over the temperature range 30–1000 K. We argue that our simple model provides a good starting point for understanding the role of local geometric effects in the physics of LiV_2O_4, and use it to explore the strength and weaknesses of three different scenarios for the magnetic "transitions" seen in this material.

Our analysis is based on the extension of a recently introduced tetragonal mean field theory to a system with a mixture of different magnetic moments. We neglect the partially itinerant nature of d-electrons in LiV_2O_4. This approximation limits the range of temperatures over which the theory is valid, but can be justified on the basis of simple physical arguments. This article is therefore divided into two parts. In Sections 2 to 4 we review and extend the mean field theory for a magnetic insulator on a pyrochlore lattice. In Section 5 we apply the generalized theory to the magnetically active V sites in LiV_2O_4, and discuss the remaining puzzles presented by the magnetic susceptibility of this most unusual material.

2 Model

2.1 The Heisenberg model on a pyrochlore lattice

The usual starting point for understanding the physics of magnetic insulators is the Heisenberg Hamiltonian

$$\mathcal{H} = \sum_{ij} J_{ij} \boldsymbol{S}_i \cdot \boldsymbol{S}_j \tag{1}$$

where $\boldsymbol{S}_i$ is the operator for the spin of electrons on site i, and the matrix element J_{ij} describes the (super-)exchange interaction between electrons on sites i and j. In this paper we consider the special case of antiferromagnetic nearest-neighbour interactions $J_{\langle ij \rangle} > 0$, on a pyrochlore lattice.

The pyrochlore lattice is a (sub-)structure common to many different magnetic insulators and a small number of metallic systems, including the sublattice of V sites in the spinel oxide LiV_2O_4. While the pyrochlore lattice has overall cubic symmetry, it can be broken down into interpenetrating A and B sublatticies of tetrahedral subunits. The bases of these tetrahedra lie in parallel planes, with

[a] e-mail: nsps@mpipks-dresden.mpg.de

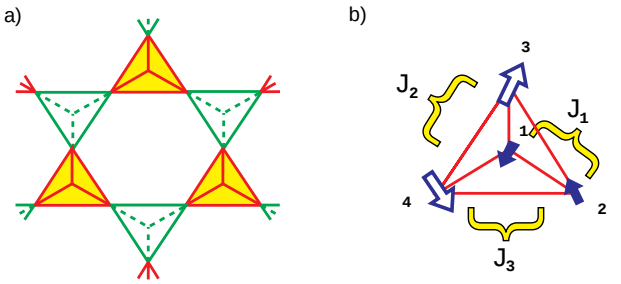

Fig. 1. a) Section of pyrochlore lattice showing two sublattice structure in terms of opposing "A" and "B" tetrahedra. In our model, spins are located at the corners of the tetrahedra and are therefore shared between the two sublattices. In this illustration, solid A sublattice tetrahedra point out of the plane, while unfilled B sublattice tetrahedra point into the plane. b) Mixed spin tetrahedron showing the different Heisenberg couplings J_1, J_2 and J_3.

the bonds in each plane forming a Kagomé lattice, as illustrated in Figure 1a. The tetrahedra of the A and B sublattices share a site at each corner, and neighbouring Kagomé planes are joined by opposing pairs of A and B sublattice tetrahedra.

In general, antiferromagnetic nearest neighbour exchange interactions favour anti-parallel spin alignments. For a bipartite lattice this presents no problem, and the classical groundstate of equation (1) is the Néel state. However the pyrochlore lattice falls into a more general class of lattices which exhibit an effect known as geometric frustration – it is impossible to construct a classical spin configuration in which all neighbouring spins are aligned anti-parallel to one another. Where this is the case, many different states can become degenerate, and geometrically frustrated magnets therefore tend to have a high (classical) ground state degeneracy. Because this degeneracy is greater than that anticipated on the basis of simple symmetry arguments, it is sometimes termed "accidental". At a classical level, such accidental degeneracies lead to the existence of new branches of zero energy excitations in addition to the true goldstone modes of the system.

Quantum and/or thermal fluctuations may enable a frustrated system to chose its true groundstate by lifting the degeneracy between different classical spin configurations [2] (equivalently, by generating a mass for all unphysical zero energy excitations). This effect falls into the broad category of "order from disorder" transitions [3]. Since calculations of order from disorder effects in quantum spin systems must take proper account of spurious classical zero energy modes, they are usually very involved (see *e.g.* [4], or for a recent example involving itinerant electrons [5]). It is therefore desirable to find a more economical way of calculating the properties of such systems. One way to do so is to start in a basis of states which already reflects the local symmetries of the lattice.

In the case of the pyrochlore lattice, where each individual tetrahedral subunit is itself geometrically frustrated, it is convenient to build up our description of the lattice starting from a basis of isolated tetrahedra.

2.2 An individual tetrahedral subunit

We start by considering an individual tetrahedron on the A sublattice:

$$\mathcal{H}_{TET} = \mathcal{H}_{EX} + \mathcal{H}_h \tag{2}$$

where $\mathcal{H}_{EX}$ the Heisenberg Hamiltonian

$$\mathcal{H}_{EX} = \sum_{\langle ij\rangle_{Tet}} J_{ij} \boldsymbol{S}_i \cdot \boldsymbol{S}_j \tag{3}$$

and in order to calculate the susceptibility we introduce an external magnetic field along the z-axis

$$\mathcal{H}_h = h \sum_i S_i^z. \tag{4}$$

Here the indices i, j denote sites at different corners of the tetrahedron, and the sum is restricted so as to count each bond between spins only once.

This subunit is a system of four interacting local moments, and we consider the case in which the magnetic ions at each corner of the tetrahedron may take on one of two possible values of total spin, these being either "large" (specifically, $S = 1$ in what follows), or "small" (below, $s = 1/2$). The exchange integral J_{ij} will in general vary with the size of the spins at sites i and j. We use the notation J_1 to refer to the exchange interaction between two small spins, J_2 to the exchange interaction between two large spins, and J_3 to the interaction between two spins of different size, as illustrated in Figure 1b. We assume that $J_2 > J_3 > J_1 > 0$, on the general grounds that more electrons contribute to exchange integrals, the larger they will be. This expectation is born out by LDA estimates of the exchange integrals J_{ij} for LiV_2O_4 [6].

Since any given tetrahedron may have 0, 1, 2, 3 or 4 large spin moments (the remainder being of the small spin) we must consider five different cases. We will not consider the additional charge degeneracy associated with the different ways of distributing spins throughout the tetrahedron as, for an insulator, this has no dynamics.

2.2.1 Excitation spectrum and partition function

Since total spin is conserved for any isolated tetrahedron, it must be possible to diagonalize the Hamiltonian (3) in the basis of eigenstates of total spin

$$\boldsymbol{\Omega} = \boldsymbol{S}_1 + \boldsymbol{S}_2 + \boldsymbol{S}_3 + \boldsymbol{S}_4 \tag{5}$$

and its z-component Ω^z. If we further introduce the total spin of the "small" and "large" spin subsystems

$$\begin{aligned} \boldsymbol{\sigma} &= \sum_{\{i\}_{Tet}} \boldsymbol{S}_i \delta_{S_i \frac{1}{2}} \\ \boldsymbol{\Sigma} &= \sum_{\{i\}_{Tet}} \boldsymbol{S}_i \delta_{S_i 1} \end{aligned} \tag{6}$$

the Hamiltonian (3) can be written

$$\mathcal{H}_{Tet} = \frac{1}{2}\left[J_\Omega \boldsymbol{\Omega}^2 + J_\sigma \boldsymbol{\sigma}^2 + J_\Sigma \boldsymbol{\Sigma}^2\right] + \text{const.} \qquad (7)$$

where $J_\Omega = J_3$, $J_\sigma = J_1 - J_3$ and $J_\Sigma = J_2 - J_3$. The coupling to external magnetic field is now simply $\mathcal{H}_h = h\Omega^z$ and the excitation spectrum of the model in the absence of a magnetic field can be read directly from the Hamiltonian (3)

$$E(\Omega,\sigma,\Sigma) = \frac{1}{2}\left[J_\Omega \Omega(\Omega+1) + J_\sigma \sigma(\sigma+1) + J_\Sigma \Sigma(\Sigma+1)\right]. \qquad (8)$$

The restriction $J_2 > J_3 > J_1 > 0$ implies that $J_\Omega > 0$, and the ground state of the tetrahedron is a spin-singlet for tetrahedra with integer total spin. Since under this assumption $J_\sigma < 0$, the smaller spins tend to be aligned in order to collectively screen the larger ones.

In order to calculate the partition function of the tetrahedron, we also need to know the degeneracy $g(\Omega,\sigma,\Sigma)$ of each state. We will not discuss the (tedious) details of the evaluation of these degeneracy factors, but note that they can be found using a simple generalization of the method introduced for systems with a single type of spin by van Vleck (see Appendix A). Actual degeneracies for the states of tetrahedra with no, one, two, three and four spin $S = 1$ spins are listed in Appendix B.

Given knowledge of $E(\Omega,\sigma,\Sigma)$ and $g(\Omega,\sigma,\Sigma)$, the partition function of the tetrahedral subunit in the presence of a magnetic field h at temperature T can be expressed as

$$Z = \sum_{\Omega\sigma\Sigma} g(\Omega,\sigma,\Sigma)\exp\left(-\frac{E(\Omega,\sigma,\Sigma)}{T}\right) \times F_\Omega\left(\frac{h\Omega}{T}\right) \qquad (9)$$

where $F_\Omega(x)$ is the function

$$F_\Omega(x) = \frac{\sinh\left(\frac{(2\Omega+1)x}{2\Omega}\right)}{\sinh\left(\frac{x}{2\Omega}\right)}. \qquad (10)$$

2.2.2 Entropy and specific heat

The entropy of an individual tetrahedral subunit is given by

$$S = \ln Z + \frac{\langle E\rangle}{T} \qquad (11)$$

where the average energy of the system $\langle E\rangle$ is

$$\langle E\rangle = \frac{1}{Z}\sum_n E_n \mathrm{e}^{-\frac{E_n}{T}}. \qquad (12)$$

The sum over states $\{n\}$ involved can easily by evaluated numerically. Results are shown in Figure 2 for the five possible mixed spin tetrahedra. For purposes of comparison, all different exchange couplings have been set equal to the single value J.

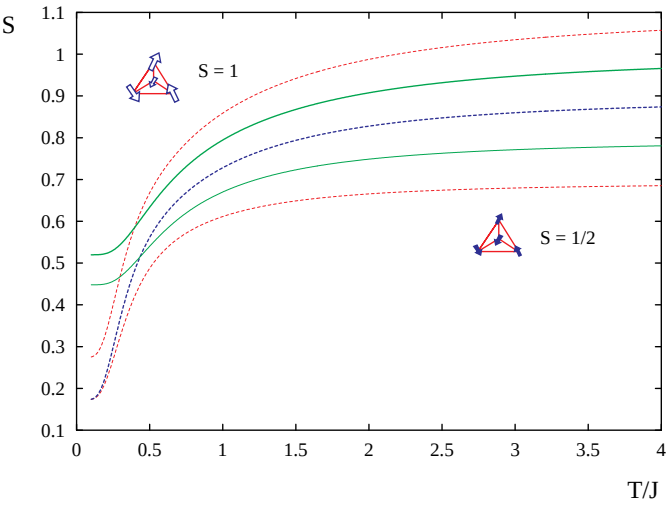

Fig. 2. Entropy of spin 1/2, spin 1 and mixed spin tetrahedra as a function of temperature in units where $k_B = 1$. From top to bottom at RHS plot, tetrahedra with – 4 spin 1 (dotted line), 3 spin 1 and 1 spin 1/2 (solid line), 2 spin 1 and 2 spin 1/2 (dotted line), 1 spin 1 and 3 spin 1/2 (solid line), 4 spin 1/2 (dotted line). All couplings set equal to J.

The entropy increases from a lower bound set by the groundstate degeneracy and tends towards an upper bound set by the total number of spin degrees of freedom for each tetrahedron. This crossover from collective ground state to individual spin degrees of freedom takes place on a scale of temperatures of order of the exchange coupling constant J, and the entropy has a point of inflection for $T \sim J/2$. A more realistic parameterization of the exchange constants $\{J_1, J_2, J_3\} \neq J$ modifies the details of the crossover, but does not affect the high or low temperature limits.

Similarly, we can evaluate the specific heat of the system

$$c_V = \frac{\langle E^2\rangle - \langle E\rangle^2}{T^2} \qquad (13)$$

in terms of its the mean square energy

$$\langle E^2\rangle = \frac{1}{Z}\sum_n E_n^2 \mathrm{e}^{-\frac{E_n}{T}}. \qquad (14)$$

Results are shown for the same set of tetrahedra in Figure 3. Once again, for purposes of comparison, all exchange constants have been set equal to J.

The heat capacity of the tetrahedra at temperatures $T \ll J$ vanishes since the first excitation energy of the tetrahedron occurs at finite energy $E_1 \sim J$. The heat capacity is peaked for $T \sim J/2$, where the entropy has its point of inflection, and tends to zero at high temperatures as the entropy of the individual spins in the tetrahedron are saturated.

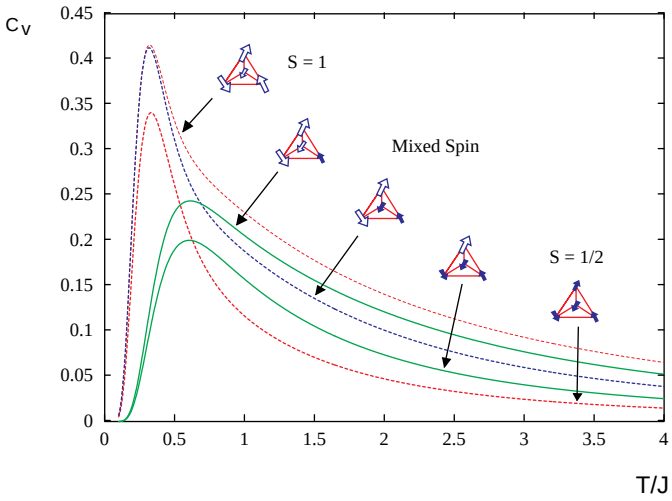

Fig. 3. Heat capacity of spin 1/2, spin 1 and mixed spin tetrahedra as a function of temperature in units where $k_B = 1$. From top to bottom at RHS plot, tetrahedra with – 4 spin 1 (dotted line), 3 spin 1 and 1 spin 1/2 (solid line), 2 spin 1 and 2 spin 1/2 (dotted line), 1 spin 1 and 3 spin 1/2 (solid line), 4 spin 1/2 (dotted line). All couplings set equal to J.

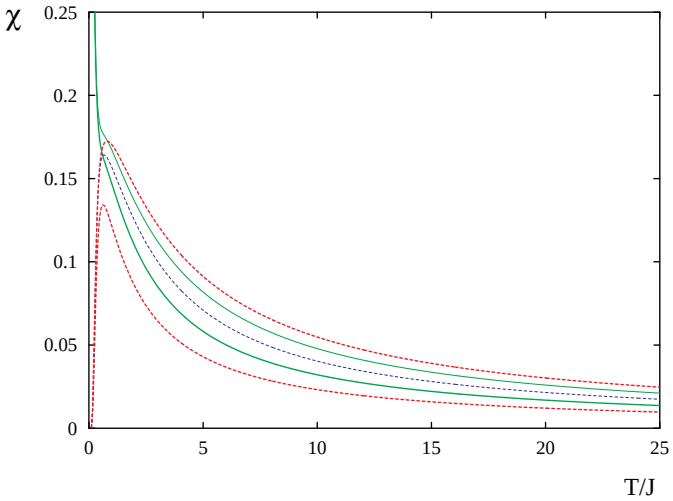

Fig. 4. Magnetic susceptibility of spin 1/2, spin 1 and mixed spin tetrahedra as a function of temperature. From top to bottom at RHS plot, tetrahedra with – 4 spin 1 (dotted line), 3 spin 1 and 1 spin 1/2 (solid line), 2 spin 1 and 2 spin 1/2 (dotted line), 1 spin 1 and 3 spin 1/2 (solid line), 4 spin 1/2 (dotted line). All couplings set equal to J.

2.2.3 Magnetic susceptibility

The magnetization of the tetrahedron in the presence of a magnetic field is given by

$$M = \frac{1}{Z}\sum_{\Omega\sigma\Sigma} g(\Omega,\sigma,\Sigma)\exp\left(-\frac{E(\Omega,\sigma,\Sigma)}{T}\right) \times \Omega F_\Omega\left(\frac{h\Omega}{T}\right) B_\Omega\left(\frac{h\Omega}{T}\right) \quad (15)$$

where $B_\Omega(x)$ is the Brillouin function

$$B_\Omega(x) = \frac{(2\Omega+1)}{2\Omega}\coth\left(\frac{(2\Omega+1)x}{2\Omega}\right) - \frac{1}{2\Omega}\coth\left(\frac{x}{2\Omega}\right). \quad (16)$$

We define the susceptibility *per site* of the tetrahedron by

$$\chi^{\mathcal{T}et}(T) = \frac{1}{4}\frac{\partial M}{\partial h} \approx \frac{1}{4}\frac{M}{h} \quad (17)$$

which in the limit of small h/T, gives

$$\chi^{\mathcal{T}et}(T) = \frac{1}{12T}\frac{1}{Z}\sum_{\Omega\sigma\Sigma} g(\Omega,\sigma,\Sigma) \times \Omega(\Omega+1)(2\Omega+1)\exp\left(-\frac{E(\Omega,\sigma,\Sigma)}{T}\right) \quad (18)$$

where, to the same level of approximation

$$Z \approx \sum_{\Omega\sigma\Sigma} g(\Omega,\sigma,\Sigma)(2\Omega+1) \times \exp\left(-\frac{E(\Omega,\sigma,\Sigma)}{T}\right). \quad (19)$$

Results for the susceptibility of the five different tetrahedra are shown in Figure 4. Once again, in order to simplify comparisons, all exchange constants have been set equal to J.

In the limit where $T/J \to \infty$ we must recover a Curie-Weiss susceptibility

$$\chi^{\mathcal{T}et}(T \to \infty) \to \frac{C}{T+\theta} \quad (20)$$

where the coefficient C represents the contribution of an individual spin to the susceptibility and θ is the Curie temperature associated with interactions between spins within the same tetrahedron. In practice the crossover to this high temperature regime occurs for $T \sim 5J$.

The value of C is given by $C_S = S(S+1)/3$ only when the tetrahedral subsystem consists entirely of spin S local moments. For the mixed spin case, it is an average of the different C_S's of the different spins within the tetrahedron. In general it can be written as

$$C = \frac{1}{12}\frac{N_1}{N_0} \quad (21)$$

where

$$N_0 = \sum_{\Omega\sigma\Sigma} g(\Omega,\sigma,\Sigma)(2\Omega+1) \quad (22)$$

is the total number of states of the system and

$$N_1 = \sum_{\Omega\sigma\Sigma} g(\Omega,\sigma,\Sigma)(2\Omega+1)\Omega(\Omega+1) \quad (23)$$

is a number determined by the degeneracy $g(\Omega,\sigma,\Sigma)$ of the states of the mixed spin tetrahedron.

Table 1. Curie coefficients and temperatures for tetrahedra with different mixtures of spin. Mean field corrections to the Curie temperature assume $z_{eff} = 3$.

	C	θ	$\Delta\theta^{\mathcal{MF}}$
$(\frac{1}{2},\frac{1}{2},\frac{1}{2},\frac{1}{2})$	0.25	$0.75J_1$	$0.75J_{eff}$
$(1,\frac{1}{2},\frac{1}{2},\frac{1}{2})$	0.351	$0.159J_1 + 0.855J_3$	
$(1,1,\frac{1}{2},\frac{1}{2})$	0.458	$0.0068J_1 + 0.485J_2 + 0.727J_3$	$1.374J_{eff}$
$(1,1,1,\frac{1}{2})$	0.558	$0.759J_2 + 0.923J_3$	
$(1,1,1,1)$	0.667	$2.00J_2$	$2.00J_{eff}$

Similarly, for a tetrahedron with a single size of spin, the Curie temperature θ associated with interaction between spins can be written $\theta_S = z_0 JS(S+1)$ where $z_0 = 3$ is the number of neighbouring spins within the same tetrahedron. In the mixed spin case, this generalizes to

$$\theta = \frac{J_\Omega}{2}\left(\frac{N_2}{N_1} - \frac{N_1}{N_0}\right) + \frac{J_\sigma}{2}\left(\frac{N_2^\sigma}{N_1} - \frac{N_1^\sigma}{N_0}\right) + \frac{J_\Sigma}{2}\left(\frac{N_2^\Sigma}{N_1} - \frac{N_1^\Sigma}{N_0}\right) \quad (24)$$

where the various numerical factors are given by

$$N_1^\sigma = \sum_{\Omega\sigma\Sigma} g(\Omega,\sigma,\Sigma)(2\Omega+1)\sigma(\sigma+1) \quad (25)$$

$$N_1^\Sigma = \sum_{\Omega\sigma\Sigma} g(\Omega,\sigma,\Sigma)(2\Omega+1)\Sigma(\Sigma+1) \quad (26)$$

$$N_2 = \sum_{\Omega\sigma\Sigma} g(\Omega,\sigma,\Sigma)(2\Omega+1)\Omega^2(\Omega+1)^2 \quad (27)$$

$$N_2^\sigma = \sum_{\Omega\sigma\Sigma} g(\Omega,\sigma,\Sigma)(2\Omega+1)\Omega(\Omega+1)\,\sigma(\sigma+1) \quad (28)$$

$$N_2^\Sigma = \sum_{\Omega\sigma\Sigma} g(\Omega,\sigma,\Sigma)(2\Omega+1)\Omega(\Omega+1)\,\Sigma(\Sigma+1). \quad (29)$$

Values of the coefficient C and the Curie temperature θ for different mixed spin tetrahedra are given in Table 1. As a compact notation we refer to a tetrahedron with one spin one and three spin half moments as $(1, 1/2, 1/2, 1/2)$, etc. The related numerical coefficients, and degeneracy factors are listed in an Appendix. Mean field corrections to θ for tetrahedra with integer total spin will be discussed below.

At low temperatures $T \ll J$ the behaviour of the susceptibility depends on the spin of the ground state of the tetrahedron. The tetrahedra with an even total spin have singlet ground states, so the lowest lying excitation which couples to magnetic fields is a triplet state at finite energy. This leads to an exponentially activated magnetic susceptibility at low temperatures, visible for the three relevant cases in Figure 4. At intermediate temperatures $T \sim J$ the susceptibility for these systems is strongly peaked, before crossing over smoothly to the anticipated Curie law at high temperatures.

The tetrahedra with an odd total spin, on the other hand, have ground states with a net spin $\Omega = 1/2$, and for $T < J$ exhibit a Curie law divergence as $\chi(T) \sim 3/12 \times T$, as seen in Figure 4. At intermediate temperatures the susceptibilities of these tetrahedra cross over smoothly to the (different) high temperature Curie-Weiss law.

The idea of calculating the magnetic susceptibility of the spin S (classical) Heisenberg model on a Pyrochlore lattice using an independent assembly of tetrahedral subunits has been previously proposed by Moessner and Berlinsky [7].

2.3 Mean field theory

As suggested by Garciá-Adeva and Huber [8], we can construct a mean field theory for the Heisenberg model on a pyrochlore lattice by considering each spin within a tetrahedron on the A sublattice to feel only the average effect of interactions with spins in other tetrahedra. Where the groundstate of each tetrahedron is assumed to be a spin singlet, for example in the three integer total spin cases considered above, the different tetrahedra interact with one another only when a magnetic field is applied. In this case, the effective field felt by any given spin is *reduced* by its AF interaction with the induced magnetization of neighbouring tetrahedra, and the susceptibility of the system is accordingly modified to

$$\chi^{\mathcal{MF}}(T) = \frac{\chi^{\mathcal{T}et}(T)}{1 + z_{eff} J_{eff} \chi^{\mathcal{T}et}(T)} \quad (30)$$

where z_{eff} is the number of neighbouring spins in *different* tetrahedra, and J_{eff} is the effective exchange interaction for the "missing" bonds of the B sublattice. In theory, for a single spin system with a single type of spin and only nearest neighbour interactions $z_{eff} = z_0 = 3$ and $J_{eff} = J$. But in practice, even for systems with only one type of spin, when it comes to comparison with experiment, the product $z_{eff} J_{eff}$ is probably best regarded as an adjustable parameter [8].

The new mean field Curie temperature is related to the Curie temperature of an isolated tetrahedron by

$$\theta_{\mathcal{MF}} = \theta + z_{eff} J_{eff} C \quad (31)$$

The coefficient C of the high temperature susceptibility is of course independent of interaction and so unchanged.

For simplicity, we have limited our discussion here to the case of tetrahedra with singlet groundstates, where the generalization of the theory presented by [8] is most straightforward. Results for the mean field susceptibilities of different tetrahedra are shown in Figure 5. For AF exchange interactions as defined above, the mean field corrections lead to an overall suppression of the susceptibility, which is reflected in the increase of the Curie temperature calculated above. The tetrahedra with an even number of spin $S = 1$ moments still show a peak in their susceptibility at $T \sim J$, but this is now a less pronounced maximum.

In the examples above we have set all the exchange constants $\{J_1, J_2, J_3, J_{eff}\} = J$. In Figure 6 we illustrate the effect of relaxing this constraint on the magnetic

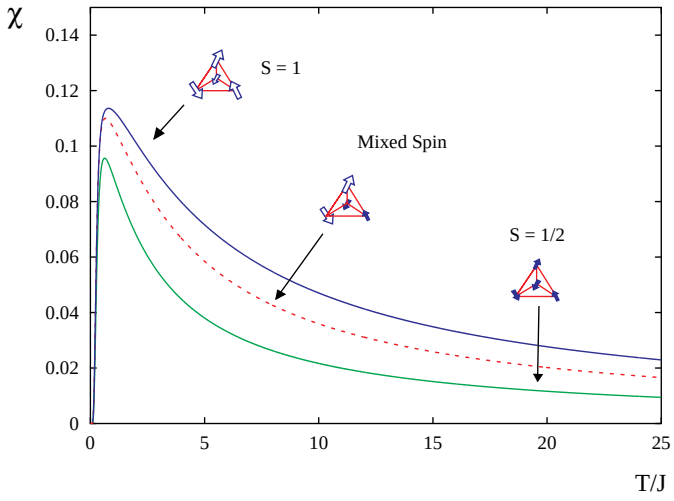

Fig. 5. Magnetic susceptibility of spin 1/2, spin 1 and mixed spin tetrahedron with two spin 1 moments as a function of temperature, including mean field interactions between tetrahedra. All couplings set equal to J.

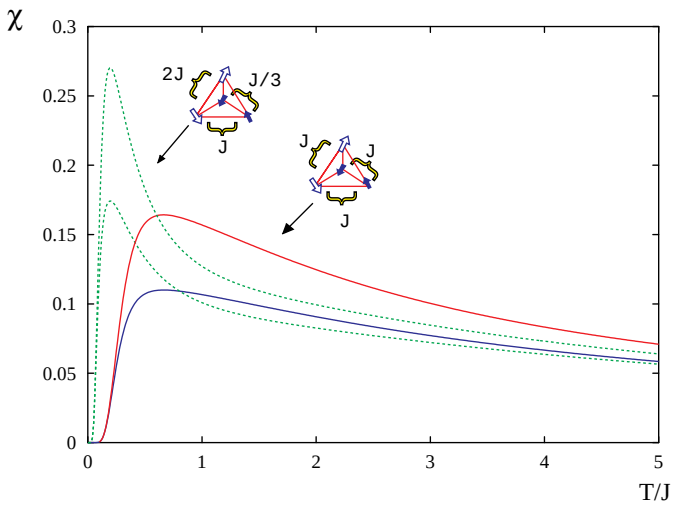

Fig. 6. Magnetic susceptibility of isolated tetrahedron with two spin 1 and two spin 1/2 (upper pair lines) and mean field susceptibility of equivalent lattice model (lower pair lines). Solid lines are for $J_1 = J_2 = J_3 = J_{eff} = J$. Dashed lines are for $J_3 = J$, $J_1 = J/3$, $J_2 = 2J$, $J_{eff} = 0.680441$, chosen so that the mean field Curie temperature is the same in each case.

susceptibility of an individual tetrahedron with two spin $S = 1$ moments, and on the mean field theory for a lattice of such tetrahedra. Lowering the coupling between the two spin $S = 1/2$ moments to $J_1 = J/3$ while increasing that between the spin $S = 1$ moments to $J_2 = 2J$ leads to a sharper peak in the susceptibility at lower temperatures, as more excitations become accessible at low temperatures.

However, since the high temperature susceptibility is of Curie law form in either case, these modifications are pronounced only on a scale of $T \sim J \to 2J$. From Table 1 we see that while the low energy scale J_1 is important for the low temperature susceptibility, the Curie temperature

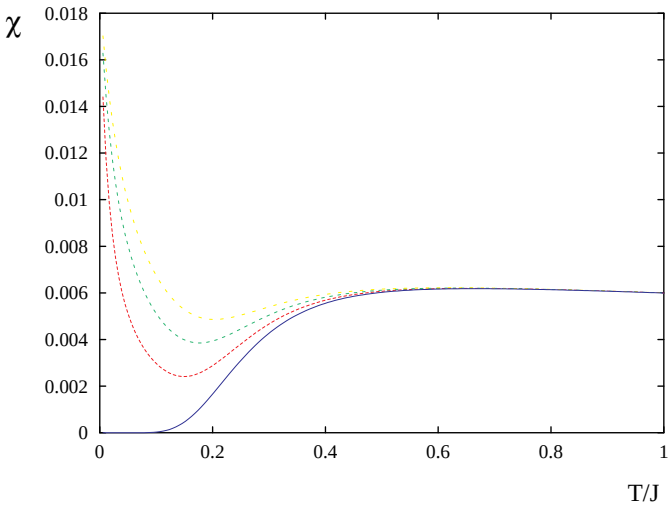

Fig. 7. Mean field theory including different types of mixed spin tetrahedra. From top to bottom – $\alpha = 0.3$ (dotted line), $\alpha = 0.2$ (dotted line), $\alpha = 0.1$ (dotted line), $\alpha = 0.0$ (solid line), where α is defined by equation (32).

of the tetrahedron is extremely insensitive to change in J_1. In the example plotted, the mean field coupling J_{eff} has been adjusted so as to compensate for the new values of J_1 and J_3, giving the same Curie temperature and therefore the same high temperature susceptibility. In practice the two models become indistinguishable for $T > 5J$. This means that a representative average "J" can be extracted from knowledge of the high temperature susceptibility of a system described by this model.

It is also interesting to consider the case of a lattice of such tetrahedra which is modified by the inclusion of a low density of "impurity" tetrahedra with greater (or lesser) total spin. To make this concrete, let us suppose that on average each tetrahedron contains two spin $S = 1$ and two spin $S = 1/2$ moments, but that in some fraction $\alpha/2$ of tetrahedra, there are in fact three spin $S = 1$ moments, and in an equal number three spin $S = 1/2$ moments. Then the mean field susceptibility is modified to

$$\chi^{\mathcal{T}et}(\alpha, T) = \alpha\chi^{\mathcal{T}et}_{(11\frac{1}{2}\frac{1}{2})}(T) + \frac{\alpha}{2}\left[\chi^{\mathcal{T}et}_{(111\frac{1}{2})}(T) + \chi^{\mathcal{T}et}_{(1\frac{1}{2}\frac{1}{2}\frac{1}{2})}(T)\right]. \quad (32)$$

Results are shown for $J_1 = J_2 = J_3 = J_{eff} = J$ and a range of values of α in Figure 7. At high temperatures the system must show its "average" character in a well defined Curie law, and the redistribution of moments between different tetrahedra is irrelevant. For temperatures $T > J/2$ the increased susceptibility of the tetrahedra with three spin $S = 1$ moments exactly cancels the reduced susceptibility of the tetrahedra with three spin $S = 1/2$ moments and all results collapse onto the curve for $\alpha = 0$. At lower temperatures the presence of the tetrahedra with a net groundstate spin leads to an upturn in the susceptibility. This becomes steadily more pronounced as $\alpha \to 1$, although the mean field theory cannot be relied upon in this limit.

Further generalizations of the mean field theory introduced in [8] for geometrically frustrated magnets with a single type of spin have been given in [9–11].

3 Magnetic susceptibility of LiV_2O_4

LiV_2O_4 is the first d-electron system to exhibit true "heavy Fermion", *i.e.* Pauli paramagnetism and (approximately) linear specific heat at low temperature, both with strongly enhanced coefficients, but with a Wilson ratio $W \sim 1.7$ [12]. The Fermi energy lies in the vanadium t_{2g} d electron bands, which are in total half filled, giving an average of 1.5 d electrons per vanadium lattice site. A presumed strong Hund's rule coupling implies that in an atomic basis, each site possesses either a spin $S = 1/2$ or spin $S = 1$ moment, according to whether one or two d-electrons are found on that site.

At very low temperatures the resistivity of LiV_2O_4 increases as T^2 [13], and the Nuclear relaxation rate obeys the Korringa law $1/T_1T = \text{const.}$, as would be expected of a Fermi liquid with well defined quasi-particles [14]. However this behaviour breaks down at about 4 K, and LiV_2O_4 is a poor conductor, with low temperature resistivity intermediate between that of a good metal (Ag, Cu) and that of an intrinsic semi-conductor (Si,Ga). In addition, the entropy associated with the low energy electronic excitations of the system is very large. An estimate made by integrating the heat capacity (after appropriate background subtractions for phonon and impurity contributions) gives approximately $0.5k_B \log 2$ per site at 50 K [13]. This value is much greater than that for any other d-electron system, and should be compared with the maximum entropy per site of $k_B \log 2$ for a single spin $S = 1/2$ degree of freedom. If we interpret the low temperature heavy Fermion behaviour of LiV_2O_4 naively in terms of an enhanced mass, electronic quasi-particles are approximately as massive as muons. Bandstructure calculations, on the other hand, suggest a relatively small mass correction and underestimate the specific coefficient γ by a factor of 25 [15,16].

At about 20 K, the electronic physics of LiV_2O_4 undergoes marked change, visible in measurements of resistivity, heat capacity, susceptibility and Hall coefficient [13]. This crossover has sometimes been identified with the coherence temperature for an s-f heavy Fermion system, and a number of authors have suggested a minimal Kondo lattice model for LiV_2O_4 in which two-thirds of the d-electrons play the role of local moments (a single spin $S = 1/2$ per site), and the remaining third are itinerant. Various mechanisms have been proposed to justify treating subsets of the vanadium t_{2g} d-electrons on a different footing, and hints of local moment physics for d electrons are even seen in some band structure calculations [16], but no real sign of Kondo physics (*e.g.* logerythmic corrections to resistivity) are seen immediately above the "transition" at 20 K.

The magnetic susceptibility of LiV_2O_4 displays a number of interesting features over a wide range of temperatures. At low temperatures ($T < 40$ K) it exhibits a weakly temperature dependent Pauli paramagnetic susceptibility, but with a massively enhanced value of $\chi \sim 5 \times 10^{-3}$ per mole vanadium. This crosses over smoothly to what has generally been interpreted as Curie law behaviour, but with different coefficients in different temperature ranges 100–500 K and 500–1000 K [17,18]. Over the same wide range of temperatures the resistivity continues to increase slowly but monotonically, and comfortably exceeds the Mott-Regel limit [13].

In what follows we will make the approximation of treating LiV_2O_4 as an insulating Heisenberg system of magnetic moments on a pyrochlore lattice. This is not unreasonable, as the magnetic susceptibility of LiV_2O_4 varies on a scale typical of Heisenberg exchange integrals (10–100 K), and not on the scale of the Hund's rule coupling or d-electron bandwidths found from LDA calculations (both $\sim 10^4$ K), and because the naive mean free path for electrons is of atomic proportions. Furthermore, the frustrated geometry of the pyrochlore lattice means that spin coherence lengths will also be small, so the tetrahedral mean field theory developed above can be expected to provide a reasonable starting point for discussing its magnetic susceptibility. In what follows we will consider three different scenarios for the magnetic physics of LiV_2O_4, using our simple model and the experimentally measured susceptibility to place constraints on each.

The theoretical predictions for magnetic susceptibility per spin given above can be related to the experimentally measured susceptibility in emu per mole vanadium (equivalently cm^3 $[\text{mol V}]^{-1}$) according to

$$\chi^{\text{exp}}(T) = 0.375 g_L^2 \chi^{\text{theory}}(T) \tag{33}$$

where $g_L \sim 2.0$ is the Landé g-factor for the coupling of a magnetic field to the spin of a vanadium ion. We note that experimental susceptibilities are often quoted in emu mol^{-1}, *i.e.* per it mole-formula-unit. One mole of LiV_2O_4 contains two vanadium ions.

3.1 First scenario – mixed valent local moments near to charge order

The vanadium atoms in LiV_2O_4 occur in two valence states, d^1 (V^{4+}) and d^2 (V^{3+}). Both of these have an incomplete shell of d-electrons, and vanadium has a strong Hund's first rule coupling, so both have a net magnetic moment – $S = 1/2$ in the case of V^{4+}, and $S = 1$ in the case of V^{3+}.

Another important fact is that LiV_2O_4 is close to charge order. This could be anticipated by analogy with other mixed valent transition metal spinels – for example those Ferrites which undergo a Verwey (charge ordering) transition. To explain this, Anderson invoked a "tetrahedron rule" requiring that charge balance be satisfied within each tetrahedron, *i.e.*, that each tetrahedron should have two of the high, and two of the low ionization states [20]. If all events violating the tetrahedron rule are neglected, a charge ordered magnetic insulating state can be stabilized by either long range interactions [20] or a distortion of the lattice [21]. The remaining dynamics

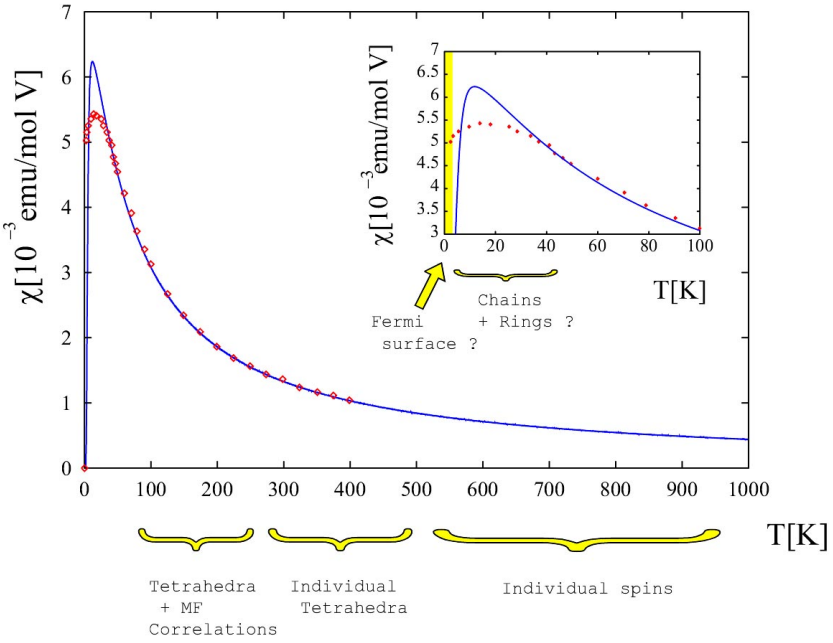

Fig. 8. First scenario – fit of mixed-spin tetragonal mean field theory to the experimentally measured magnetic susceptibility of LiV_2O_4 over the temperature range 0–400 K, taken from [19], using the two adjustable parameters $g = 1.6$ and $J = 17.8$ K. Annotation on the temperature axis shows the type of correlation between spins. Inset – how the fit breaks down at low temperatures. A possible interpretation of the electronic state of the system in terms of charge order correlations in different low temperature ranges is given.

are then determined by the residual (antiferromagnetic) Heisenberg exchange integrals.

While LDA estimates suggest that the energy associated with Coulomb interaction between V^{3+} and V^{4+} ions on neighbouring sites is lower than the threshold for charge order [22], experimentally LiV_2O_4 *does* charge order under pressure [23]. It has therefore been suggested by Fulde *et al.* [6] that the application of the tetrahedron rule to LiV_2O_4 provides a way of explaining its heavy Fermion behaviour at low temperatures.

The essential ingredient of this theory is the emergence of one-dimensional correlations between spins as a result of the tetrahedron rule. Since each tetrahedron has two spin one and two spin half moments, every vanadium atom must be connected to two vanadium atoms with same moment, one within its tetrahedron, and one in a neighbouring tetrahedron. This means that the lattice of tetrahedra can be divided into Heisenberg chains of spin half or spin one moments. These chains may close to form rings, with a minimum length of six spins. The remaining simplification is that the interaction between neighbouring chains is neglected, so that the spin one chains have (Haldane-)gapped excitations, while the spin half chains have low lying fermionic excitations (spinons) with linear specific heat. These, and not the dressed electronic quasiparticles of the more familiar rare earth heavy Fermion compounds, are the heavy Fermions of Fulde's theory.

Since this scenario for calculating the low temperature susceptibility of LiV_2O_4 is based on the tetrahedron rule, and treats LiV_2O_4 as an insulator, it is natural to extend it to higher temperatures using the tetragonal mean field theory for a mixed valent system described above. Specifically, the tetrahedron with two spin one and two spin half moments considered in Section 2 corresponds *exactly* to a tetrahedral subunit of four neighbouring V atoms in LiV_2O_4, on the assumption that charge balance is achieved locally by including two V^{4+} and two V^{3+} in each tetrahedron, in accordance with Anderson's tetrahedron rule. It is this four spin elementary unit, which has a integer total spin and therefore a singlet groundstate, that will form the basis of our mean field theory.

Both the mean field and the Fulde spinon theories have singlet groundstates, but in the mean field theory the triplet excitations which couple to magnetic field have no dispersion and therefore retain a finite excitation energy J_3. The spinon theory, on the other hand, includes (approximately) the processes which lift this degeneracy, and captures the low lying excitations necessary to explain the Pauli paramagnetism and linear specific heat of LiV_2O_4. The two theories will therefore disagree in their predictions at very low temperatures, but must agree in the high temperature limit for which local moment physics is recovered. The mean field theory is essentially exact for the wide range of temperatures for which the range of magnetic correlations on the pyrochlore lattice does not extend beyond an individual tetrahedron [7].

Figure 8 shows a mean field fit to the experimental susceptibility of LiV_2O_4 taken from [19], based on tetrahedra with two spin one and two spin half moments. The fit is excellent down to temperatures of order 20–30 K, at which one might expect correlation effects beyond the scope of a mean field theory (for example the formation

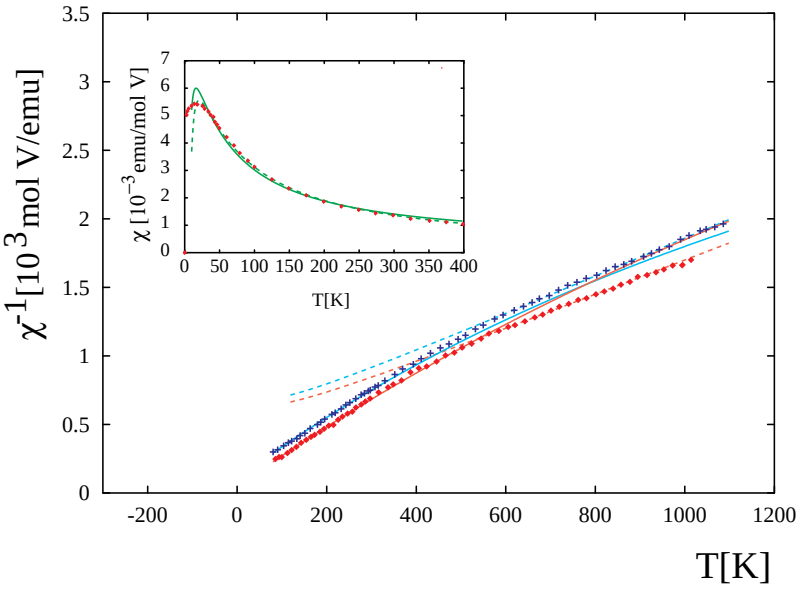

Fig. 9. Second scenario – inverse magnetic susceptibility of LiV_2O_4 over the range 0–1100 K as quoted in [17] (diamonds), [18] (squares), together with linear fits to the "Curie Law" behaviour seen at high (broken lines) and low temperatures (unbroken lines). Inset – low temperature fit to susceptibility taken from [19], assuming a lattice of spin 1/2 moments and Landé g-factor $g = 2.04$ (solid line), together with unconstrained fit (broken line).

of chains and rings), and above all the fact that LiV_2O_4 is not an insulator, to become important.

Two adjustable parameters have been used for the fit, the Landé g-factor g_L and a single representative Heisenberg exchange integral $J = J_1 = J_2 = J_3 = J_{eff}$. The effective correlation number z_{eff} is set equal to three. The parameters g_L and J are then uniquely determined by the Curie temperature $\theta = 47$ K and coefficient $C = 0.46$ K emu/mol V which can be extracted from the Curie law behaviour of the susceptibility on the range 100–400 K. The fit below 100 K then provides an independent test of the validity of the tetragonal mean field theory. As can be seen in the inset to Figure 8, the tetragonal mean field theory appears to be very successful, at least over the range of temperatures for which it can reasonably be applied.

It is tempting to identify the temperature $T \sim J \approx 20$ K at which both the model and experimental susceptibilities have their maximum, and begin to diverge, as the scale for a crossover to a new low temperature state. It is almost certainly true that the inclusion of processes which violated the tetrahedron rule, *i.e.* the hopping of electrons between tetrahedra, prevent the system from achieving the local singlet groundstate on which the mean field theory is based, and might reasonably lead to the emergence of a HF state. This, within Fulde's scenario, would occur through the deconfinement of spinons.

However, even above 40 K, where the fit is very good, a number of important experimental facts remain unaddressed by this scenario. One is that the Landé g-factor extracted from the fit is really too low, $g_L = 1.6$, as compared with the usual value of $g_L = 2.0$ found for bulk Vanadium. The tetrahedral mean field theory also has too great an entropy, and therefore too great a heat capacity as compared with experimental estimates. But the most challenging observation is that published susceptibility data for temperatures of order 1000 K appear to show a crossover to a different Curie law regime with $C \approx 700$ K emu/mol V and $\theta \approx 400$ K. It is this issue which we address in the following section.

3.2 Second scenario – two different local moment regimes

Figure 9 shows the *inverse* magnetic susceptibility of LiV_2O_4 between 100 and 1100 K, as reported by Muhtar *et al.* [17] and Hayakawa *et al.* [18]. Above 600 K, and below 400 K Curie law behaviour is seen in the sense that the inverse susceptibility can be approximated by a straight line with slope $1/C$ and intercept θ. However the values of the Curie temperature θ and the the coefficient C are quite different for the high and low temperature regimes.

In fact the value of the C found at high temperatures corresponds quite well to that which would be expected for an equal mixture of spin half and spin one moments (V^{4+} and V^{3+} ions), assuming a Landé factor $g_L = 2.0$, while the value of C found at low temperatures is much closer to that which would be expected if each tetrahedral site had a spin half moment.

This has prompted the suggestion that the full spin moment of the V atoms is seen only at high temperatures, while at lower temperatures this moment is partially "screened" by correlations between spins in such a way that only a net spin of one half remains at each V site (see *e.g.* [24]). The majority of theoretical attempts to explain heavy Fermion behaviour in LiV_2O_4 [24–28] take as a starting point a tetrahedral lattice of spin half moments

Table 2. Exchange coefficients, exponents, and Landé g-factors found from fits to data.

	Kondo *et al.* [19]	Muhtar *et al.* [17]	Hayakawa *et al.* [18]
First scenario:			
g_L	1.6	–	–
J	17.8 K	–	–
Second scenario – high temperature regime:			
g_L	–	2.04	2.14
J	–	119 K	122 K
Second scenario – low temperature regime:			
χ_0	0.26×10^{-3} emu/mol V	0.18×10^{-3} emu/mol V	0.12×10^{-3} emu/mol V
J	26 K	25 K	13 K
Third scenario:			
α	–	0.74	0.80
T_0	–	0.021	0.053

(often identified with the A_{1g} representation of the V d-electron states), and assign the remaining half an electron per site to an itinerant electron band (equivalently, E_g states). We will not attempt to review these theories here, but in the light of these models, it is clearly worth trying to obtain a "self consistent" fit to both the high and low temperature magnetic susceptibilities of LiV_2O_4 within the overall scenario of two local moment regimes.

Using the tetragonal mean field theory developed above, we therefore proceed as follows: we first (least squares) fit the high temperature (600–1000 K) susceptibility assuming an equal mixture of spin one and spin half moments, using the two adjustable parameters J and g_L, as described in the previous analysis. We obtain values of $g_L = 2.04$ and $J = 119$ K for data taken from Muhtar *et al.* [17] with a mean square error per point of $\sigma = 0.0028$ emu/mol V, as recorded in Table 2. Similarly, for data taken from Hayakawa *et al.* [18] we obtain $g_L = 2.14$, $J = 122$ K and $\sigma = 0.0024$ emu/mol V. Then, using the value of the Landé g-factor g_L obtained at high temperatures, we fit the low temperature susceptibility (100–400 K). We do this assuming that each tetrahedral site has a localized spin half moment, and that the contribution of the remaining itinerant electrons can be lumped into a single paramagnetic constant χ_0 so that

$$\chi(T) = \chi_0 + \chi^{\mathcal{MF}}(T) \tag{34}$$

where $\chi^{\mathcal{MF}}(T)$ is the mean field susceptibility of the lattice of spin half lattice tetrahedra [29]. As fit parameters we use χ_0 and J, the exchange integral between the local spin half moments. We obtain values $\chi_0 = 0.18$ emu/mol V and $J = 25$ K with an error $\sigma = 0.030$ for data taken from Muhtar *et al.* [17] and $\chi_0 = 0.12$ emu/mol V, $J = 13$ K and $\sigma = 0.047$ emu/mol V for data taken from Hayakawa *et al.* [18].

In Figure 9 we plot the data described above, showing the high temperature fit with dashed and the low temperature fit with unbroken lines. Each fit is good, within its own domain of validity. The values of the fit parameters obtained from data taken from [17] and [18] are not quite the same, and the apparent variation in values of the Landé g-factor g_L might be a cause for concern. However, as the fit parameters strongly depend on the how background contributions were subtracted from the experimental data, it is difficult to draw any strong conclusions about their precise values, and note the absolute values of susceptibility quoted for the heavy Fermion phase of LiV_2O_4 at very low temperatures also vary from group to group.

In the inset to Figure 9 we show fits to the low temperature susceptibility of LiV_2O_4 as measured by [19] on the range 40–400 K, using a model susceptibility of the form equation (34). As no high temperature data was available for this sample, we use both constrained (solid line) and unconstrained (dashed line) values of g_L. Values of the fit parameters are shown in Table 2. For the constrained fit a value of $g_L = 2.04$ was taken from high temperature data for [17], using which values of $\chi_0 = 0.26$ emu/mol V and $J = 26.0$ K were found, with a mean square error per point of $\sigma = 0.11$ emu/mol V. The better fit was in fact obtained for the unconstrained (three parameter) fit, for which $\chi_0 = 0$ emu/mol V, $J = 33$ K and $g_L = 2.3$, and $\sigma = 0.052$ emu/mol V.

To summarize, the assumption that LiV_2O_4 has two different local moment regimes as a function of temperature, leads to fits to its magnetic susceptibility which a) have physically parameters and b) have an error comparable to the uncertainty of the data. However, by splitting the data into different temperature regimes in this way we have not only assigned a physical meaning to the observed change in the slope of the inverse susceptibility, but also diminished what we learn from each fit – almost any data set could be fitted piecewise, but cutting it into small enough pieces. Most importantly, our mean field theory can tell us nothing about how such a crossover between different local moment regimes takes place, and this remains an important question for microscopic theories of LiV_2O_4 to address.

In the section below we consider a radically different, and admittedly speculative, way of understanding the

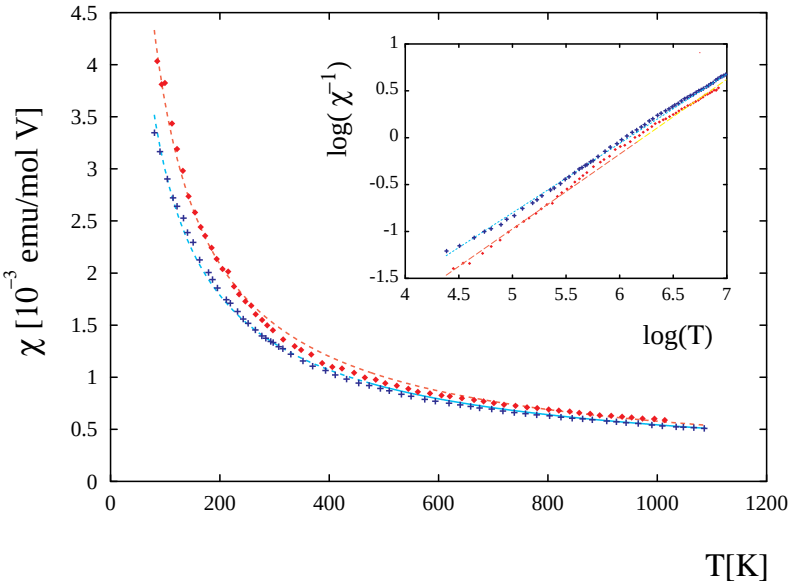

Fig. 10. Third scenario – power law fits to the magnetic susceptibility of LiV_2O_4 as measured by [17] (diamonds) and [18] (crosses), with exponents of 0.74 and 0.80, respectively. Inset – inverse susceptibility and power law fits plotted on a log-log scale.

magnetic susceptibility of LiV_2O_4 over the temperature range 100–1100 K, prompted by experiments on Zn and Li doped samples.

3.3 Third scenario – powerlaw scaling

LiV_2O_4 is by no means the only spinel oxide. Many different systems have been synthesized, and all possess the same geometric frustration, which leads to a complex interplay of spin, charge and orbital order, which may in turn be linked to lattice modes [21]. This is evident in the many different ground states which these systems achieve – some like $ZnCr_2O_4$ stabilizing spin order through a distortion of the lattice, others, like AlV_2O_4, achieving charge order through valence skipping. Crudely speaking, each material seeks a means of reducing the high entropy associated with its frustrated geometry by playing off different competing forms of order. In LiV_2O_4 the low temperature state is a heavy Fermi liquid, and it seems reasonable to believe that the system is a poor metal precisely because no one form of insulating order is achieved.

It is possible to dope LiV_2O_4 by substituting the Zn for Li to give $Li_{1-x}Zn_xV_2O_4$ [17], or by substituting Ti for V to give $LiTi_yV_{2-y}O_4$ [18]. Zn is a magnetic impurity, and occupies the octahedral sites in the spinel. The inclusion of small concentrations of Zn forces LiV_2O_4 into a spin glass phase, with a spin glass temperature which vanishes as the number of Zn impurities tends to zero [13]. The alternative "parent" compound $Zn_1V_2O_4$ is an AF Mott insulator. Ti is non-magnetic, and occupies tetrahedral sites in the spinel. Small concentrations of Ti do not substantially alter the properties of LiV_2O_4, but at larger dopings it undergoes a metal insulator transition. $LiTi_2O_4$ is a conventional superconductor with $T_c = 13.7$ K. The Curie coefficient C extracted from the high temperature susceptibilities of $Li_{1-x}Zn_xV_2O_4$ and $LiTi_yV_{2-y}O_4$ does appear to have the expected dependence on doping.

So LiV_2O_4 lies at a quantum critical point for a transition into a spin glass phase on doping, and is close to charge order on the application of pressure. It is therefore clear that there is quantum phase transition (probably, a line of critical points) close to the undoped, ambient pressure, ground state. What influence, if any, could this be expected to have? Quantum phase transitions at zero temperature can manifest themselves at finite temperature through the power law scaling of response functions. Is there any evidence for scaling behaviour in LiV_2O_4?

We make the simple conjecture that the magnetic susceptibility of LiV_2O_4 might be described by a simple power law of the form

$$\chi(T) = A\left(\frac{T}{T_0}\right)^{\alpha} \tag{35}$$

over a wide range of temperatures.

The magnetic susceptibility of LiV_2O_4 is shown plotted on a log-log scale in the inset to Figure 10. If the temperature dependence of the data were a simple power law, the data would lie on a straight line. In the case of a Curie law, this straight line would have a gradient of one.

A least squares fit to the susceptibility data reported by [17] *over the full range of temperatures* (*i.e.* 100–1100 K) leads to an exponent $\alpha = 0.74$, with a mean error per point of $\sigma = 0.038$. In the case of the data reported by [18], fitting the full data set from 100–1000 K, we find an exponent $\alpha = 0.80$, and an error per point $\sigma = 0.053$. The errors of these fits are not as good as those for the fits to Curie law behaviour at high temperatures, but no worse than those for the self consistent low temperature fits within the two local moment scenario. The fits are shown on a linear scale in Figure 10.

Existing evidence therefore does not rule out the possibility that, rather than exhibiting a crossover between two different local moment regimes, the magnetic susceptibility of LiV_2O_4 has a simple power law behaviour over a very wide range of temperatures. Such powerlaw scaling would eventually have to "saturate" in Curie law behaviour at very high temperatures, when correlations between moments can legitimately be ignored.

4 Conclusions

The magnetic susceptibility of the heavy Fermion spinel LiV_2O_4 is puzzeling, not only in the size of the paramagnetic contribution found at low temperatures, but in the way in which this crosses over to local moment behaviour at high temperatures. We consider geometric frustration to play an important role LiV_2O_4 and have addressed this issue by extending a recently introduced tetragonal mean field theory for a Heisenberg model on a pyrochlore lattice to allow for mixed valance.

Using this theory as a tool to make comparison with the experimentally measured magnetic susceptibility of LiV_2O_4, we have considered a number of different scenarios for the crossover from (roughly) temperature indpendant paramagnetism below 40 K to apparent Curie law behaviour at 1000 K. We find that fits based on the tetragonal mean field theory work well below 400 K, for a wide range of parameter sets, suggesting that the geometry of the lattice plays an important role in determining the magnetic properties of LiV_2O_4. However not all of these fits yield physically reasonable values of the Landé g-factor and so the low temperature susceptibility alone cannot uniquely constrain the model used.

Considering the susceptibility from 100–1100 K, we find that fits based on the assumption of two different local moment regimes, and fits based on the ansatz of power law scaling, both provide a reasonable account of the data. This leads us to speculate that instability of LiV_2O_4 against a spin glass state (on doping), and a charge ordered state (under pressure) manifests itself a the non-analytic behaviour of the magnetic susceptibility.

Further analysis of theory and experiment is needed to distinguish between these scenarios.

It is our pleasure to acknowledge the suggestions and encouragement of Peter Fulde, together with helpful conversations with David Huber, Sinchiro Kondo, Hide Takagi and Victor Yushanghi. We would also like thank Martin Albrecht for a careful reading of the manuscript. This work was supported under the visitors program of MPI-PKS.

Appendix A: Degeneracy of a state with total spin Ω

The problem of how to find the degeneracy of a state with total spin $\Omega \leq NS$ of a system of n spins of length S was solved by Van Vleck [30]. Here we review his derivation, which may then be generalized easily to a system of mixed spin.

We first consider the simpler problem of finding $g^z(M)$, the number of states of the system with z-component of total spin $\Omega^z = M$. By simple combinatorics, this is given by the coefficient of x^M in the polynomial

$$\left(x^S + x^{S-1} + \ldots + x^{-S}\right)^n. \tag{36}$$

The first few terms in this series are easy to calculate and have obvious physical significance. They also demonstrate the pattern for finding further terms

$$x^{nS} \to \left(x^S\right)^n \to 1 \tag{37}$$

$$x^{(n-1)S} \to \left(x^S\right)^{(n-1)} \times 1 \to n \tag{38}$$

$$x^{(n-1)S} \to \left(x^S\right)^{(n-2)} \times 1 \times 1 + \left(x^S\right)^{(n-1)} \times \left(x^{-S}\right)^{(n-1)} \to \frac{n!}{(n-2)!2!} + \frac{n!}{(n-1)!1!}. \tag{39}$$

If we consider instead a system of n_1 spins of size S_1 and n_1 spins of size S_2 the polynomial in question becomes

$$\left(x^{S_1} + x^{S_1-1} + \ldots + x^{-S_1}\right)^{n_1} \times \left(x^{S_2} + x^{S_2-1} + \ldots + x^{-S_2}\right)^{n_2}. \tag{40}$$

For the purposes of calculating the partition function of a tetrahedron what we need is $g(\Omega)$, the number of possible states with total spin Ω, and not $g^z(M)$, the number of states with $\Omega^z = M$. We find $g(\Omega)$ by setting up a difference equation. The number of possible states $g^z(M)$ with magnetization $M > 0$ must increase with decreasing M, since all states with total spin $\Omega \geq M$ contribute to $g^z(M)$. It follows immediately that the required degeneracy $g(\Omega)$ is just the rate of change of $g^z(M)$ for $M = \Omega$, *i.e.*

$$g(\Omega) = g^z(\Omega) - g^z(\Omega + 1). \tag{41}$$

This generalizes directly to the case of a mixed spin system.

Appendix B: Degeneracies $\mathbf{g}(\Omega, \sigma, \Sigma)$

Table 3. Degeneracy $g(\Omega)$ for states of spin $S = 1/2$ tetrahedron with total spin Ω and values of associated coefficients.

	$\Omega = 0$	$\Omega = 1$	$\Omega = 2$
$S = 1/2$	2	3	1
N_0	16		
N_1	48		
N_2	216		

Table 4. Degeneracy $g(\Omega, \sigma)$ for states of tetrahedron with three $S = 1/2$ and one $S = 1$ spins as function of total spin $\Omega = \{1/2, 3/2, 5/2\}$, spin of $S = 1/2$ subsystem $\sigma = \{1/2, 3/2\}$, and values of associated coefficients.

	$\sigma = 1/2$	$\sigma = 3/2$
$\Omega = 1/2$	1	2
$\Omega = 3/2$	1	2
$\Omega = 5/2$	0	1
N_0	24	
N_1	101	
N_1^σ	71	
N_2	630	
N_2^σ	331	

Table 5. Degeneracy $g(\Omega, \sigma, \Sigma)$ for states of tetrahedron with two $S = 1/2$ and two $S = 1$ spins as function of total spin $\Omega = \{0, 1, 2, 3\}$, spin of $S = 1/2$ subsystem $\sigma = \{0, 1\}$ and spin of $S = 1$ subsystem $\Sigma = \{0, 1, 2\}$, and values of associated coefficients.

$\Omega = 0$	$\sigma = 0$	$\sigma = 1$
$\Sigma = 0$	1	0
$\Sigma = 1$	0	1
$\Sigma = 2$	0	0
$\Omega = 1$	$\sigma = 0$	$\sigma = 1$
$\Sigma = 0$	0	1
$\Sigma = 1$	1	1
$\Sigma = 2$	0	1
$\Omega = 2$	$\sigma = 0$	$\sigma = 1$
$\Sigma = 0$	0	0
$\Sigma = 1$	0	1
$\Sigma = 2$	1	1
$\Omega = 3$	$\sigma = 0$	$\sigma = 1$
$\Sigma = 0$	0	0
$\Sigma = 1$	0	0
$\Sigma = 2$	0	1
N_0	36	
N_1	198	
N_1^σ	54	
N_1^Σ	144	
N_2	1596	
N_2^σ	324	
N_2^Σ	984	

Table 6. Degeneracy $g(\Omega, \Sigma)$ for states of tetrahedron with one $S = 1/2$ and three $S = 1$ spins as function of total spin $\Omega = \{1/2, 3/2, 5/2, 7/2\}$, and spin of $S = 1$ subsystem $\Sigma = \{0, 1, 2, 3\}$, and values of associated coefficients.

	$\Sigma = 0$	$\Sigma = 1$	$\Sigma = 2$	$\Sigma = 3$
$\Omega = 1/2$	1	1	1	1
$\Omega = 3/2$	0	1	2	2
$\Omega = 5/2$	0	0	1	2
$\Omega = 7/2$	0	0	0	1
N_0	54			
N_1	362			
N_1^Σ	468			
N_2	3645			
N_2^Σ	3687			

Table 7. Degeneracy $g(\Omega)$ for states of spin $S = 1$ tetrahedron with total spin Ω and values of associated coefficients.

	$\Omega = 0$	$\Omega = 1$	$\Omega = 2$	$\Omega = 3$	$\Omega = 4$
S=1	3	6	6	3	1
N_0	81				
N_1	648				
N_2	776				

References

1. R. Moessner, *Key-note theory talk of Conference on Highly Frustrated Magnetism (HFM-2000) in Waterloo, Canada, June 2000*, `cond-mat/0010301`
2. E.F. Shender, JETP **56**, 178 (1982)
3. J. Villain, Z. Phys. B **33**, 31 (1979)
4. A.V. Chubukov, Phys. Rev. Lett. **69**, 832 (1979)
5. N. Shannon, A.V. Chubukov, J. Phys. Cond. Matt. **14**, L235 (2002)
6. P. Fulde *et al.*, Europhys. Lett. **54**, 779 (2001)
7. R. Moessner, A.J. Berlinsky, Phys. Rev. Lett. **83**, 3293 (1999)
8. A.J. Garciá-Adeva, D.L. Huber, Phys. Rev. Lett. **85** 4598 (2000)
9. A.J. Garciá-Adeva, D.L. Huber, Phys. Rev. B **63**, 174433 (2001)
10. A.J. Garciá-Adeva, D.L. Huber, Phys. Rev. B **63**, R140404 (2001)
11. A.J. Garciá-Adeva, D.L. Huber, Phys. Rev. B **65**, 184418 (2002)
12. S. Kondo *et al.*, Phys. Rev. Lett. **78**, 3729 (1997)
13. C. Urano *et al.*, Phys. Rev. Lett. **85**, 1052 (2000)
14. A.V. Mahajan *et al.*, Phys. Rev. B **57**, 8890 (1998)
15. See *e.g.* J. Matsuno *et al.*, Phys. Rev. B **60**, 1607 (1999)
16. D. Singh *et al.*, Phys. Rev. B **60**, 16359 (1999)
17. Muhtar *et al.*, J. Phys. Soc. Jpn **57**, 3119 (1988)
18. Muhtar *et al.*, J. Phys. Soc. Jpn **58**, 2867 (1989)
19. S. Kondo *et al.*, Phys. Rev. B **59**, 2609 (1999)
20. P.W. Anderson, Phys. Rev. **102**, 1008 (1956)
21. See *e.g.* O. Tschernyshyov, R. Moessner, S.L. Sondhi, Phys. Rev. Lett. **88**, 67203 (2002)
22. A.N. Yaresko, private communication, 2001

23. H. Takagi, private communication, 2001
24. J. Hopkinson, P. Coleman, preprint, cond-mat/0203288
25. V.I. Asinimov *et al.*, Phys. Rev. Lett. **83**, 364 (1999)
26. C. Varma, Phys. Rev. B **60**, R6973 (1999)
27. C. Lacroix, *Proceedings of HFM-Conference, June 2000, Waterloo, Ontario, Canada*, to appear in Can. J. Phys., cond-mat/0107574
28. M.S. Laad *et al.*, preprint, cond-mat/0202531
29. We have checked that includind the constant term χ_0 self consistantly in the mean field term does not alter the fits in any meaningful way
30. J.H. van Vleck, *The theory of electric and magnetic susceptibilities* (Oxford, 1932)